Reliability Improvements in Repair Welding of High-strength Steels` IIW Doc IX-2002-01

Dr.sc. Ivan Samardžić*
Dr. Thomas Siewert **

* Dr.sc. Ivan Samardžić, Mechanical Engineering Faculty in Slavonski Brod (CROATIA)
** Dr. Thomas Siewert, National Institute for Standards and Technology, Boulder (Colorado,USA)

Key words: degradation, high-strength steels, reliability improvement, repair welding

Summary: Engineers often have to deal with repair of weldments after they have been put into service. Here, the concern is that the service environment may have changed the structure, independent of whether the problems originated during the initial construction (cold and hot cracks, inclusions, porosity, etc.) or during subsequent service (wear, damage, stress-corrosion cracking, etc.). In the case where the material characteristics have changed, the welding procedures used during the original construction may no longer be appropriate. Thus, it is necessary to create a new welding procedure qualification to define the specific details for an appropriate repair. In this paper, emphasis is given to repair welding of railway tanks manufactured from high-strength steels.

1. Introduction

The weld joint typically has a higher risk of failure than the rest of the structure (e.g. a weld degradation factor "V" of less than 1 is often used in calculations) [1-6]. One reason for this is that one or more properties of the base material near the weld could have degraded by the process of welding, leading to a failure through a dominant failure mode (the failure that has the greatest probability of appearing, such as stress-corrosion cracking). The failure risk might further increase if repair welding is performed. Therefore, the welding, quality control, and quality assurance technologies need to be developed to more stringent requirements if we want to avoid the conditions for failure, and so achieve higher reliability for welded construction. We are often faced with dilemmas during repair welding:

- Do the reliability requirements for the welded construction even permit repair welding?
- How many times can repair welds be performed at one place?
- Which technology should be used to produce higher reliability and less degradation at the welding joints?

In some cases, there are standards that provide answers, or inspectors (with appropriate authority) who can offer an opinion. In other cases there are not.

Different kinds of welding flaws can appear at repair welds, but the most serious are cracks. They can be characterized by location, orientation, type, size, etc.

This paper deals with possible problems that could occur during repair welding of TStE 420, a high-strength steel (HSS) that is used to manufacture pressure vessels for storage and transport of liquefied gases. The following sections describe different aspects of the problem: why repair welds have a greater variation in cooling rate (than production welds), why this variation in cooling rate leads to a greater range in hardness, and why this range in hardness leads to poorer properties in aggressive environments, such as cathodic polarization. The starting point of the discussion (and key to the problem) is the complex temperature field that occurs during repair welding, and which can cause significant degradation of the welded-joint zone (such as a decrease in the reliability of the zone of the repair weld).

2. Degradation in properties due to the complex temperature field during welding

The thermal cycles associated with the joining of two plates by welding can degrade the properties of the material adjacent to the weld. The degree of degradation is dependent on many factors, and there are several reasons why repair welds may exhibit greater degradation [7-9].
For example, repair welds are usually short, so their temperature fields are more complex than long welds (the simple 2-D temperature models apply only to semi-infinite welds). The degradation is most severe at weld starts and stops, but can also occur at other locations along the weld and for different stress conditions (welding of hybrid materials, uneven thicknesses, near the plate end, etc.). The choice of the welding process also determines the temperature field, due to the heat input into the material from the moving heat source. Accordingly, we may find a very complex temperature field inside the material. Also, there will be transition areas where the temperature fields may respond in a manner that is intermediate between the 2-D and 3-D results, depending on the boundary conditions or the start conditions. A stable temperature gradient is established after a short time for suitable dimensions around a moving heat source in a long weld. In transition areas, the cooling rate varies, so the mechanical properties can be significantly different from the areas with 2-D heat flows (areas that are quite distant from weld starts and stops). Because the temperature fields in the transition regions are so complex and because the effects are more extreme near the ends, this report will concentrate on the weld starts and stops.

The degradation in properties at weld starts and stops occurs for both long and short arc welds. It is of greater concern in short welds, because the proportion of the weld that experiences the 3-D heat-flow conditions is larger. This is shown schematically in Figure 1, which presents the cooling rate variation (w, K/s) and cooling time in welded joints (over the temperature interval from 800 ºC to 500 ºC). In the transition area of the weld joint (some area betweeen the ends and the middle), the heat flow (and so cooling rate) is intermediate. At the end of the weld (after a length of 2-D heat flow near the middle of the weld), the 3-D temperature field is present again. Since the cooling time and cooling rate of the welded joint influence the mechanical properties (such as the hardness and strength) of the welded joint, they should be kept within required margins so that any serious degradation of the mechanical properties in the transition areas at weld starts and weld stops can be avoided.

The length of the transition regions depends mainly on the heat flow of the heat source and its effective energy input, but depends also on material thickness, physical properties of material, preheating temperature, temperature between phases, etc..

In some cases, this problem can be avoided by the use of weld-on/weld-off plates that are mounted before welding and removed after welding. However, in most repair welds, mounting of weld-on/weld-off plates is not possible, so the transition or non-stationary (weld start and weld stop) areas remain in the structure.

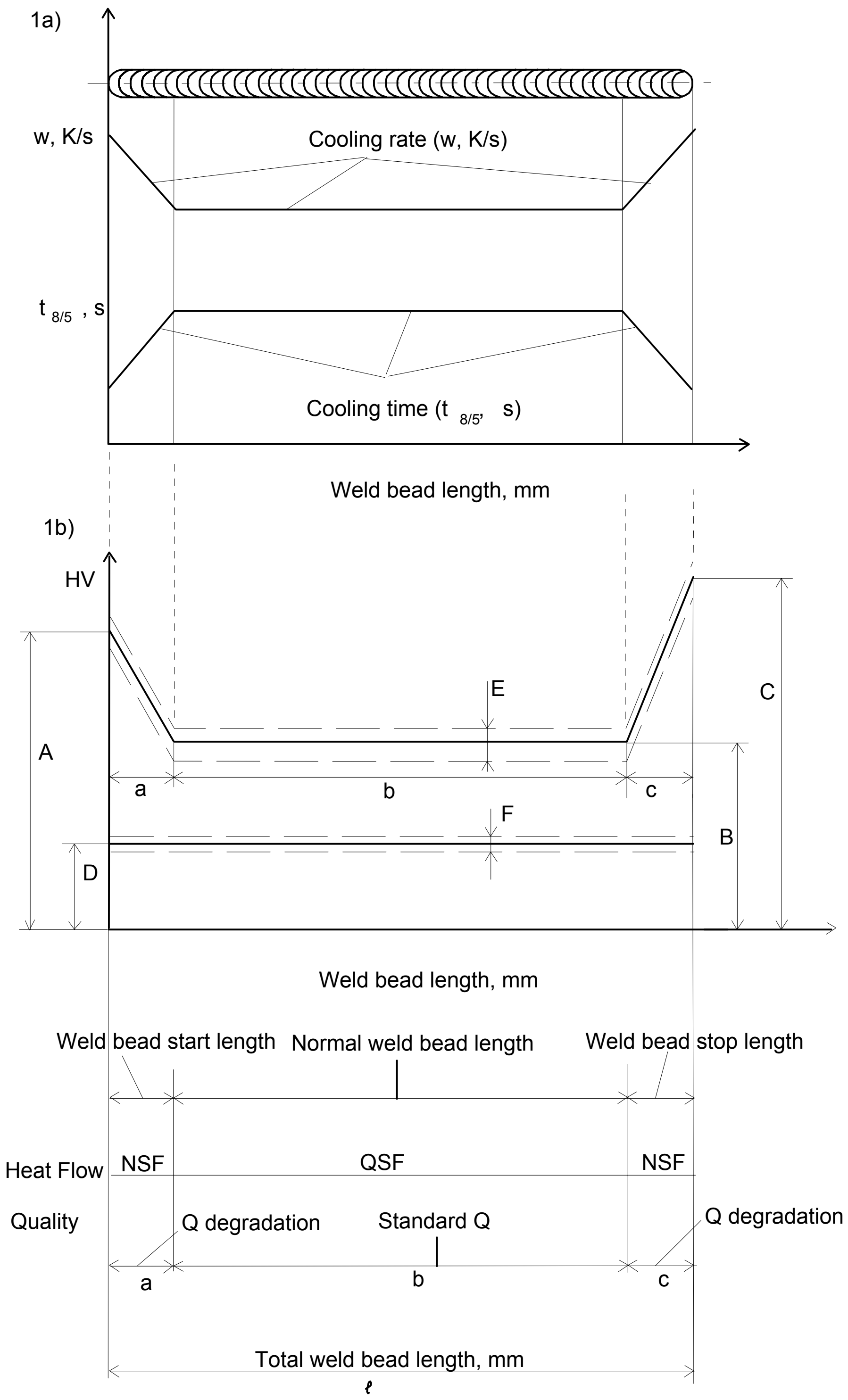

A... maximal hardness mean value at weld bead start length "a"
B... mean hardness value at normal bead length "b"
C... maximal hardness mean value at weld bead stop length "c"
D... mean hardness value in base metal
E... hardness scattering of normal bead length "b"
F... hardness scattering of base metal
NSF...non-stationary (3-D) heat flow
QSF.. quasi-stationary (2-D) heat flow
Q ... quality

Figure 1. Definitions - theoretical diagrams of variations of influencing factors on weld quality along the bead length for: cooling rate w, K/s (1a), cooling time $t_{8/5}$, s (1a) and hardness value HV (1b).

2.1. Determination of hardness differences in the heat affected zone (HAZ) along the welded joint

A series of welds was produced to investigate the effect of hardness gradients on the expected mechanical properties of the welds. The welds were produced by a number of processes (GMAW, SAW, and surfacing) on HSS with yield strengths up to 500 MPa. After test plates were welded and surfaced by controlled welding parameters, specimens were prepared for hardness measurements (HV1, HV5, HV10), microstructural analysis, and corrosion testing. A schematic view of the specimen preparation after welding of HSS steel TStE 420 is presented in Figure 2. Two characteristic diagrams were drawn from the data showing the distribution of hardness HV5 along the HAZ near the fusion line after surfacing of a plate with a thickness of 15 mm (Figures 3 and 4). The hardness was measured by the contour method [10].

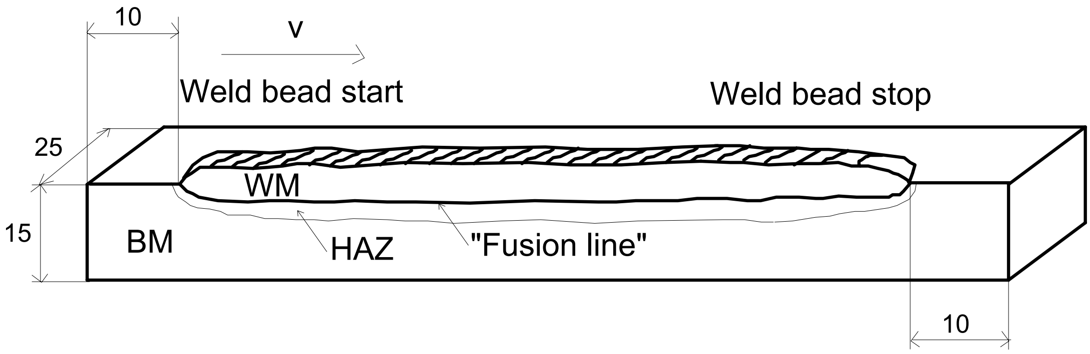

Figure 2. Schematic of specimen preparation after welding of HSS steel TStE 420.

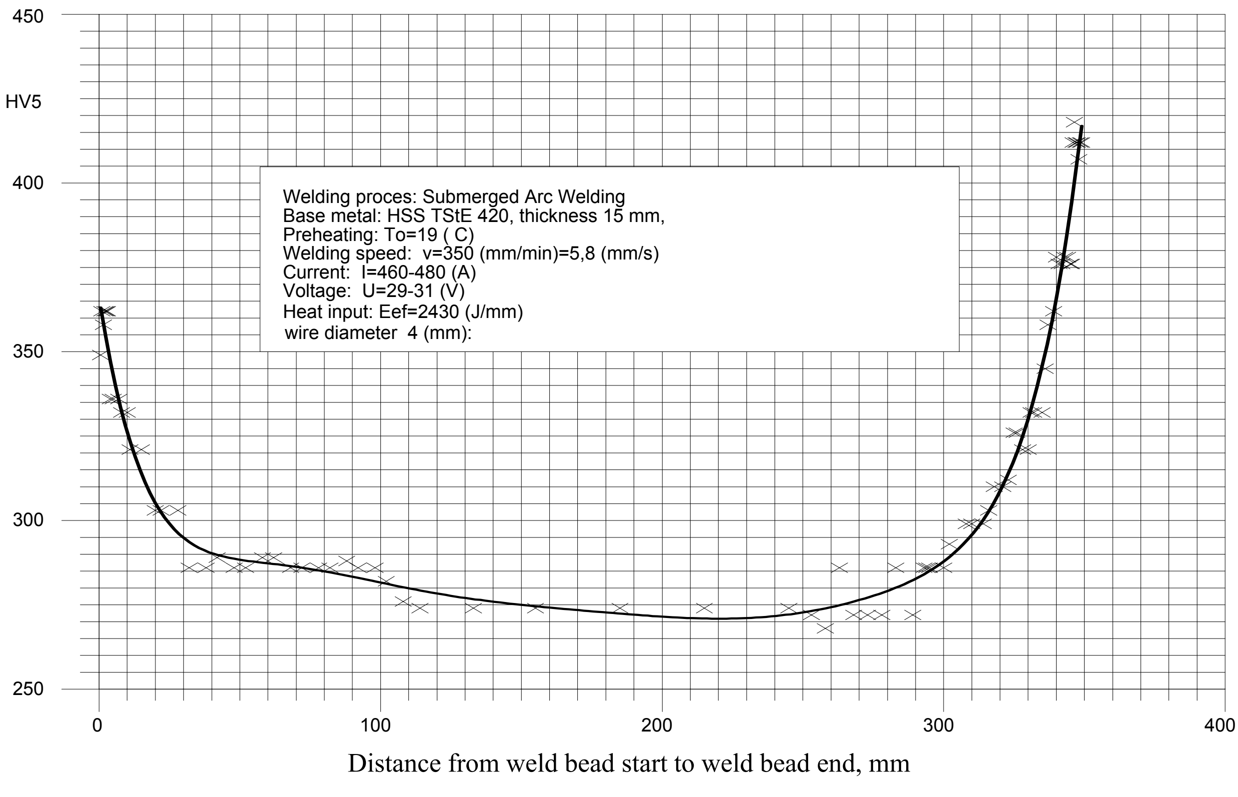

Figure 3. Hardness HV5 in the heat affected zone along the fusion line from weld start to weld end. The solid line shows the average. Welding process: submerged arc welding, base metal: TStE 420, δ=15 mm, filler metal wire diameter: ∅4 mm.

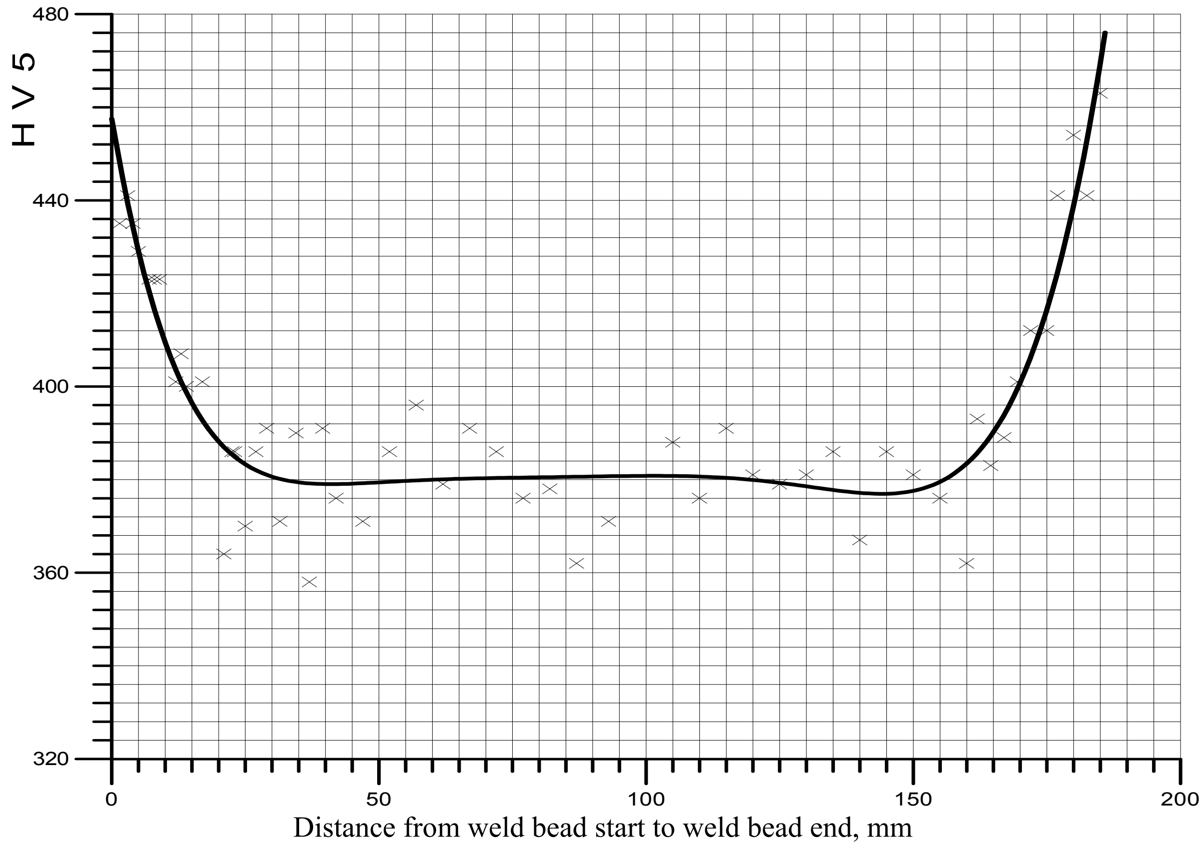

Figure 4. Hardness HV5 in the heat-affected zone along the fusion line from weld start to weld end. Welding process: manual arc welding, base metal: TStE 420, δ=15mm, filler electrode: Fox 2,5Ni, diameter: 3,25 mm, T_o=20 ºC, I=125.3 A (σ=15.6), U=22.9 V (σ=4.76), v=3,7 mm/s. Specimen G2.

Figures 3 and 4 show an increase in hardness at the weld start and stop regions, compared to the middle of the weld.

Higher values of hardness were always noticed at the end of the weld compared to those at the start. A similar distribution of hardness in the HAZ along the fusion line was noticed on all samples (30 samples), but the hardness values varied due to different welding parameters, such as heat input. Variation in the heat input changed the cooling rate, i.e. the time to cool from 800 to 500 ºC.

Based on these investigations, the influence of cooling rate in the weld joint could be analysed for the example of an experimental arc strike shown in Figure 5. An arc strike was produced with an SMAW electrode (simulation of an improper procedure) on a fine-grain steel TStE 420. Hardness measurements in the weld region showed an increased hardness over that of the base material, which is very important because this material is used for pressure vessels that are used in aggressive environments (subject to stress corrosion).

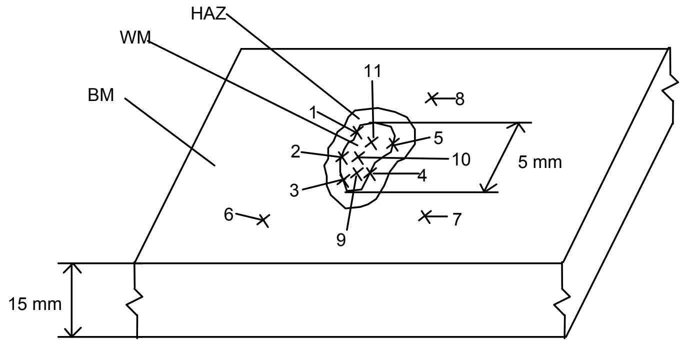

Mark	Location	HV5
1	HAZ	473
2	HAZ	466
3	HAZ	473
4	HAZ	473
5	HAZ	466
6	BM	190
7	BM	195
8	BM	185
9	WM	391
10	WM	380
11	WM	396

Figure 5. Hardness HV5 results in HAZ, along the fusion line, in WM and BM after producing an “arc strike” in steel TStE 420 (simulation of improper procedures).

At locations with higher hardness (weld starts and stops, arc strikes, ...), a stronger inclination to cracking (cold cracks) and stress corrosion is expected.

2.2. Experimental investigation of degradation at weld starts and stops

We investigated the degradation of properties at weld starts and stops, for comparison to the weld center and to the base material. This continues earlier laboratory investigations of the sensitivity to stress corrosion of weld joints and base material made from high-strength steel Nioval 50. Those investigations concluded that the parameters that determine the severity of stress corrosion are: maximum hardness in the weld joint, aggressive media, and the strength level. [11, 12, 13] In the present experiments, the base material TStE 420 was studied. The composition of steel TStE is presented in Table 1, while the principal mechanical properties are presented in Tables 2 and 3.

Table 1 Composition of base material [14].

Steel - TStE 420	C	Si	Mn	P	S	Ni	N	Al	V
Our measurements	0,15	0,38	1,46	0,017	0,005	0,22	0,018	0,023	0,13
Steel producer data	0,15	0,36	1,52	0,013	0,006	0,21	0,016	0,016	0,14

Table 2 Basic mechanical properties, from manufacturer's documentation [14].

Steel TStE 420	Yield point R_t (MPa) for different plate thicknesses (mm)				Strength R_m	Elongation, A_5, %	Bending, α=180^o	
	≤10	11-15	16-25	≥25 ≤35	MPa		Long.	Trans.
Our data	-	503	-	-	604	A_5=27 Z=61,9%	-	-
Data from the steel mill	420	420	410	410	530-680	17	3a	4a

Table 3 Basic toughness (J) [14].

Steel	Rolling Direction	Non aged				
		Temperature, ^{o}C				
		+20	0	-20	-40	-50
TStE 420	Longitudinal	63	55	47	31	27
	Transversal	39	31	27	20	16

Results of laboratory investigation of Charpy V at temperatures 20, 0, -20, and -40 ºC are as follows. [14]

Temperature 20 ^{o}C: arithmetic mean K_V=203 J (individual values: 209 J, 195 J and 205 J)
Temperature 0 ^{o}C: arithmetic mean K_V=190 J (individual values: 183 J, 196 J and 193 J)
Temperature -20 ^{o}C: arithmetic mean K_V=191 J (individual values: 196 J, 182 J and 196 J)
Temperature -40 ^{o}C: arithmetic mean K_V=163 J (individual values: 168 J, 156 J and 167 J)

2.3 Design of experiments

The surfacing of three plates (dimensions 500 mm x 250 mm x 15 mm) was predicted through a design of experiments. After weld surfacing (and recording the welding parameters and preheating temperatures), three specimens were produced for testing of hydrogen embrittlement. As shown in Figure 6, one specimen had the weld-pass start in the middle of the test section (P), one had the weld centered in the test section (S), and one had the weld stop in the middle of the test section (K). To show the tendency of the base material to stress corrosion, three specimens were also made from plate that was not surfaced.

One specimen was taken out of every four groups of specimen types (base material, weld-pass start, half of weld pass, weld-pass end) as a reference. These specimens were not exposed to hydrogen.

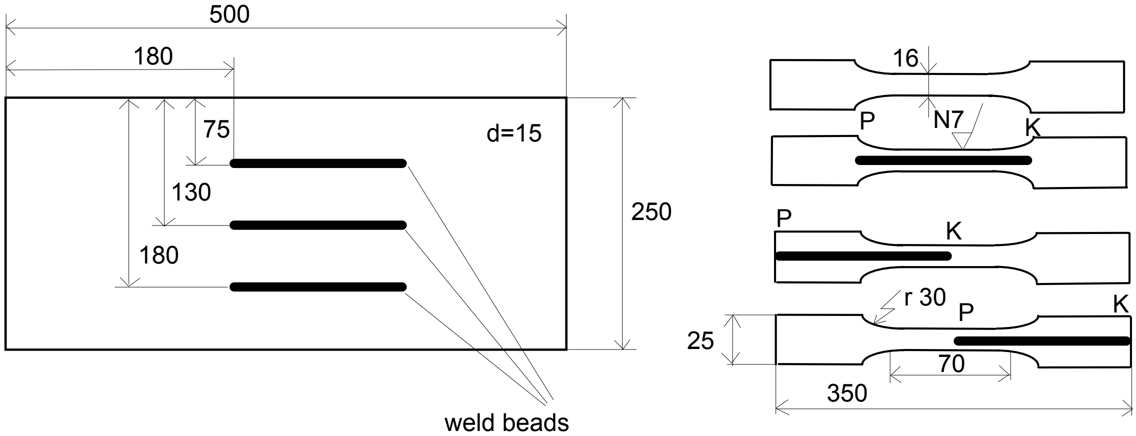

P... weld bead start
K... weld bead stop

Figure 6. Testing plates after welding (bead on plate). Two plates with 3 passes each, and one plate without welded beads – only base metal.

2.4 Surfacing

Surfacing was performed using an MAW basic electrode, Fox 2.5 Ni, diameter 3.25 mm. The temperature of the plates before surfacing was 15 ºC. Welding parameters were recorded by an on-line monitor. Average values of the surfacing parameters are listed in Table 4.

Specimens for hydrogen brittleness testing were machined from the plates. The specimens were identified according to bead location, as listed in Table 4.

Table 4. Arithmetic mean for welding parameters

	Plate 1			Plate 2		
Bead mark	3	4	5	6	7	8
Current, A	23	21,4	22,4	22,3	22,1	21,8
Voltage, V	140	138	134	136	133	140
Bead length, l_i	185	182	180	175	180	180
Welding time, s	64	63	60	55	61	60
Welding speed, mm/s	2,9	2,9	3	3,2	3	3
Heat input, J/mm	1110	1022	1000	954	996	1017

2.5 Exposing the specimens to hydrogen and fracture by tensile test of the specimens.

To evaluate the tendency of the base material, weld start, weld end, and middle section of the weld to hydrogen embrittlement, the cathodic polarization technique was used. As described in references [15], [16], [17] and [18], the presence of atomic hydrogen in a material leads to decreased plasticity. Due to differences in microstructure between the weld zones, different levels of embrittlement are expected, as a function of the base material and the weld location. Cathodic polarization was performed with a current density of 40 mA/cm^2 for 24 hours, without any stress on the specimens. The solution was 0,5 mol H_2SO_4 + 10 mg As_2O_3 per dm^3, deaerated by nitrogen for 30 minutes before cathodic polarization. Hydrogen-charged specimens were pulled on a tensile test machine with a deformation speed of 0,24 mm/s. After testing, the IK index was calculated by the formula:

$$F = \frac{Z - Z(H)}{Z} \cdot 100\% \quad \text{..........} \quad (1),$$

where:

Z ... reduction in area of uncharged specimen of base metal (used as a reference value), and

$Z(H)$ ... reduction in area of a hydrogen-charged specimen.

2.6 Results

The mechanical properties of the hydrogen-charged specimens are presented in Table 5.

Table 5. Mechanical properties of hydrogen charged (CP) specimens

Specimen	Cathodic polarization (CP)	R_e MPa	R_m MPa	A_5 %	Z %	IK	Remark
1	Base Material (BM)	503	604	27,0	61,9		Base metal
2	BM+CP	519	613	23,0	29,2	52,8	Base metal, hydrogen charged
3	Weld Middle (S)	493*	653*	14,4	28,5		Middle of bead
4	S+CP	531*	582*	8,8	20,5	66,9	Middle of bead, hydrogen charged
5	Weld Stop (K)	522	608	17,7	60,1		Bead stop
6	K+CP	490	534	18,0	12,2	80,3	Bead stop, hydrogen charged
7	Weld start (P)	477	599	18,0	61,7		Bead start
8	P+CP	497	575	9,7	16,6	73,1	Bead start, hydrogen charged

Based on square specimen area.

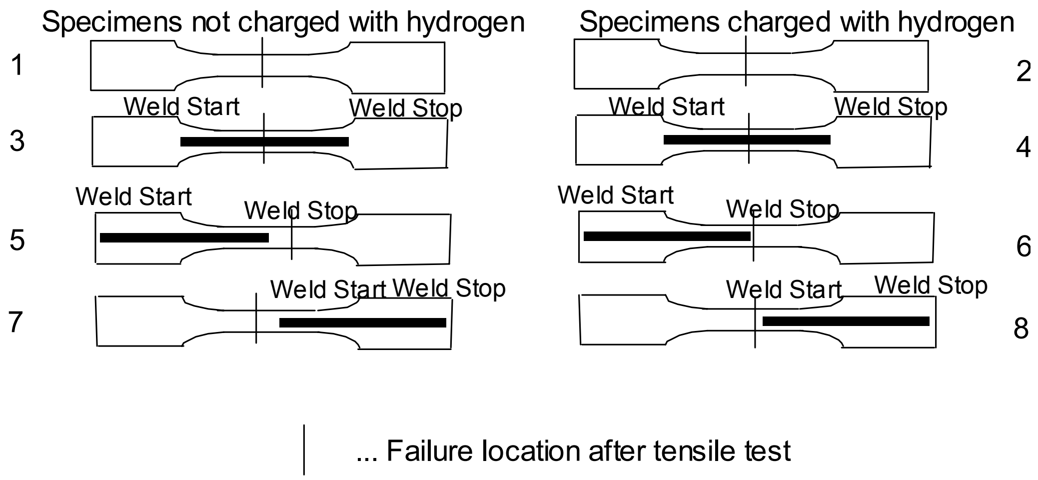

Figure 7. Failure locations after tensile testing

Figure 7 shows the location of fractures in the specimens. In specimens that had been treated with hydrogen, the fracture occured at the weld starts and stops; for the specimens not treated with hydrogen, the fracture occured at approximately 25 mm from the weld stop, i.e. in the base material.

Values of the brittleness index (IK) were obtained from formula 1. Comparison of the different values of IK shows that the smallest value of IK occurs for the base material. The middle of the weld has a lower value of IK index than the weld starts and stops. Therefore, the middle of the weld is more resistant to hydrogen embrittlement than the weld starts or stops. Comparison of the weld starts with the stops shows that the weld stop is more sensitive to hydrogen.

We were also able to develop some relationships between the IK values and the maximum hardness in the HAZ adjacent to the fusion line. Regions with higher hardness have higher inclination to hydrogen enbrittlement, i.e., higher degradation of base material due to welding.

This investigation confirms our thesis of an embrittlement of the weld starts and stops. A tendency to greater stress corrosion with an increase in maximum hardness values in the weld was also noted.

3. A short review of repair welding and repair welding techniques

Welding is used to repair manufacturing errors during construction, as well as for field repair of damaged welded structures that have been in service. However, a discussion of the concerns of repair welds is seldom found in the literature. This problem is most serious for pressure vessels working in aggressive media. Experience on railway tanks and spherical tanks shows that a large number of stress corrosion cracks have occured on poor-quality repair welds [11]. Therefore, the problem needs more investigation and analysis than ever before.

A half-bead technique is usually proposed for high-strength steels. The authors' experience suggests that this technique cannot be easily applied to weld repairs produced with SMAW because the distance from the annealing bead to the melting line must be 1 mm to 3 mm (Figure 8, detail “A”). But, when it is applied, then it is important to implement this technique on both the weld starts and stops. Correct implementation of this technique requires adequately trained welders. The maximum hardness can be decreased by increasing the preheating and reheating temperature, which could be useful for weld starts and stops. The results of experimental repair welding depend on the way in which weld starts and stops are placed in the melting zone of a previous weld.

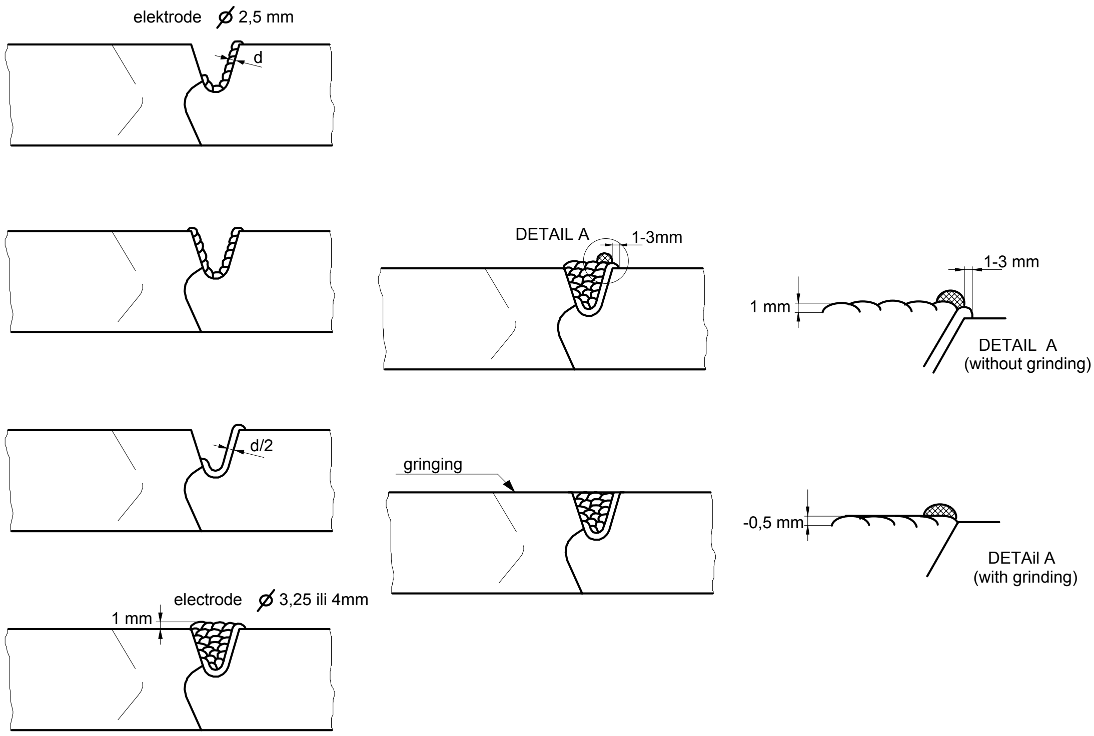

Figure 8. Weld bead sequences during repair welding using "half bead technique" [19].

4. Experimental repair welding

Repair welding was performed on plates of 15 mm thickness, with the parameters and welding techniques used during the welding of 10 railway tanks of capacity 110 m^3. Figure 9 is a schematic representation of the groove preparation. The sequences of the passes are presented in figures 10 and 11.

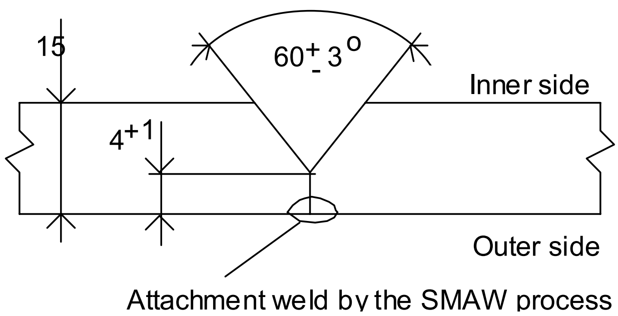

Figure 9. Preparation of a weld joint in production railway tanks.

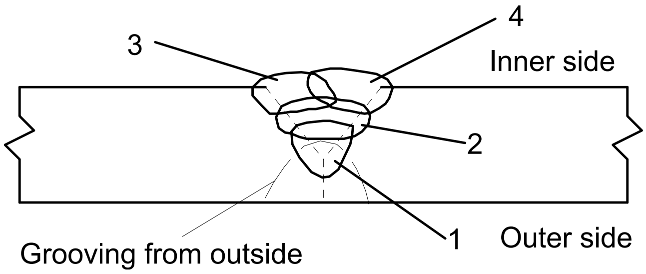

Figure 10. SAW from inside of tank, followed by grooving from outside

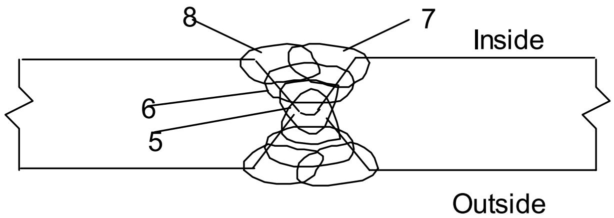

Figure 11. SAW from outside of tank, after grooving.

Table 6. Welding parameters for SAW process for each pass.

Pass	Current I, A	Voltage U, V	Wire feed v, mm/s	Preheating temp., ^{o}C	Heat input $\bar{E}$, J/mm
1	400-460	20-26	420	80	1413
2	440-460	28-30	420	80	1780
3	440-470	27-30	420	85	1853
4	440-470	27-30	420	80	1853
5	460-490	24-27	400	60-70	1817
6	440-470	25-28	440	80	1644
7	440-480	25-29	450	100	1625
8	440-470	26-30	450	105	1699

To evaluate the repair procedure, a longitidunal crack was assumed to be present in the HAZ along the melting line at a depth of 8 mm and for a length of 100 mm. A repair groove was cut with a carbon electrode and a “V” groove joint was prepared by grinding (groove angle of 60 º, radius in groove root was approximately 6 mm).

To achieve lower values of the hardness in the repair welds, the weld starts and stops were placed in the melted zone of the previous weld.
(figure 12).

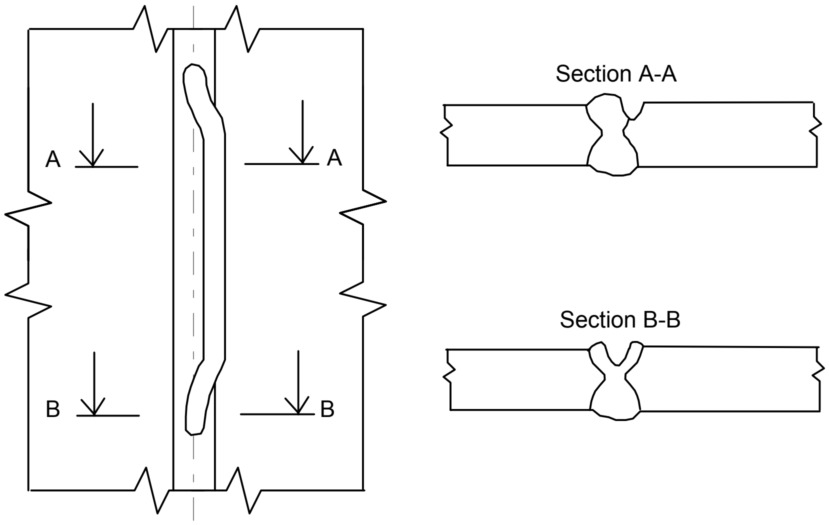

Figure 12. Repair welding - weld pass start and weld pass stop placed in the previous weld metal.

Repair welding was performed by SMAW with a Fox 2.5 Ni electrode, 3.25 mm in diameter. The preheating and interpass temperatures were kept between 150 and 200 ºC. The average heat input was 1000 J/mm. After cooling of the test plate, specimens were cut from the weld start, middle and weld end to measure the hardness (HV5). The hardnesses for the weld start and stop regions are presented in the next figure.

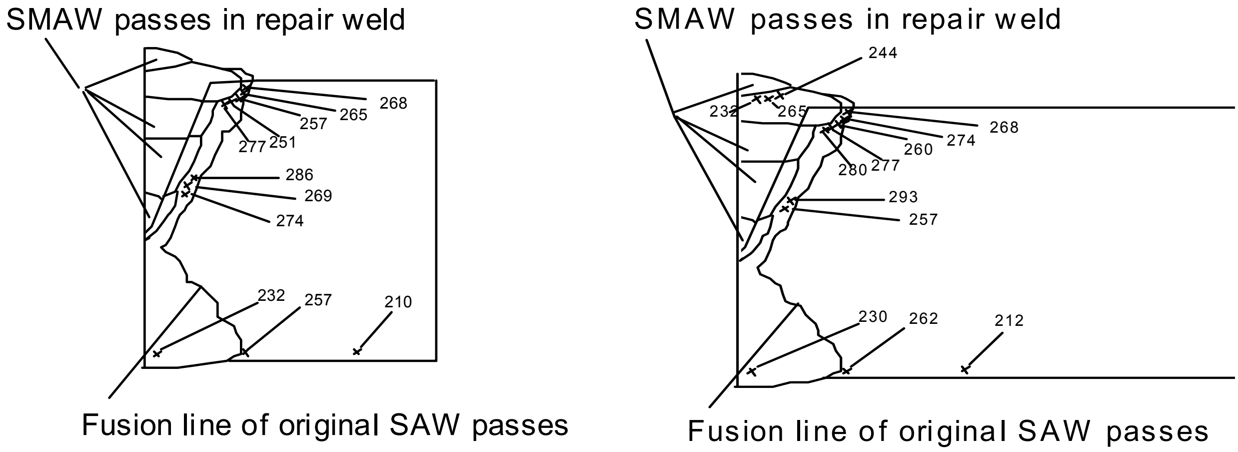

Figure 13. Maximum hardness value at TStE 420 steel repair weld start (a) stop (b).

These experimental investigations confirmed our expectation that the hardness would not increase significantly. The hardness values at the weld starts and stops were not statistically different from those for the middle of the welds.

5. Conclusion

It is important to consider the problems of differing temperature fields when approving welding procedures, especially for the weld starts and stops. The number of weld starts and stops should be minimized, and the remaining starts and stops should be designed and implemented in ways that the embrittlement is minimized. To assess the overall reliability of a structure, the properties of all weld repair regions (start, middle, and stop) must be determined. Only with such a complete knowledge of the properties can the goal of increased reliabilty of welded structures be reached. Beside general conclusions on weld starts and stops, this paper provides specific data for the repair welding of HSS TStE 420.

References:

1. *Lukačević, Z., Samardžić, I.* Weldability analysis based on probabilistic approach to reliability and weakening of welded joints. 3rd International Seminar "Numerical Analysis of Weldability", Graz-Seggau, Austria, 25-27 September 1995.
2. *Lukačević, Z.* Probabilistic Weld Efficiency and Reliability Approach for Pressure Vessels. IIW Doc. XI-407-82.
3. *Lukačević, Z.* Weld Efficiency, Reliability and Classes of Weld Joints (Philosophy on Weld Efficiencies). IIW-XI-374-80.
4. *Lukačević, Z.* Quantification of weldability, joint efficiency and reliability. Proceedings of the International Conference on the Joining of Materials - JOM-7. The European Institute for the Joining of Materials. Helsing∅r, Denmark, 1995.
5. *Lukačević, Z.* Reliability Assessment of Welded Products. Proceedings of the International Welding Conference. CMES. Hangzhou, China, 1984.
6. *Lukačević, Z., Samardžić, I.* Approach to weldments reliability modeling. The International Welding Conference, Japan-Slovak Welding Symposium, Kozice (Slovak Republic), 5-6 March 1996.
7. *Samardžić, I.* Temperature fields application in weld repair technique. Proceedings of the 19 th International Welding Congress, Bratislava, 1994, 311-321.
8. *Samardžić, I. Stoić, A.* Weakening due to temperature field variation during welding. The International Welding Conference, Japan-Slovak Welding Symposium, Kozice (Slovak Republic), 5-6 March 1996.
9. *Samardžić, I., Galović, A., Galović, M.* Nonstationary temperature fields at welding. Croatian Welding Journal “Zavarivanje” 36, 6, 1993, 211-217.
10. *Mraz, L.* Hardness measurement in underbead HAZ of single pass welds; Doc IIW IX-1609-90; 1-39.
11. *Belić, A., Lukačević, Z., Samardžić, I.* Accelerated tests for stress corrosion of welded joints. Croatian Welding Journal “Zavarivanje” 36, 4-5, 1993, 155-163.
12. *Gayk, W.* Empfehlungen zur Werkstoffauswahl und zu den Schweissdaten fur NH_3- Lagerbehalter und NH_3- Kesselwagen, Mat.-wiss u. Werkstofftech. 19, 1988, 126-132.
13. *Crackwell, A.* Stress corrosion cracking of steels in ammonia, The Institute of Refrigeration, London 1988.
14. *Gojić, M. Malina, J. Ivaniš, K.* Evaluation of hydrogen embrittlement resistance of duplex stainless steel for the oil industry. Oil (Nafta) 43 (6) 313-321, 1992, (in Croatian).
15. Base and filler metal producer certificates. Quality control department of factory PHTTV, Đuro Đaković d.o.o., Slavonski Brod, 1995, (in Croatian).
16. *Chavane, A. Habashi, M. G. M.* Pressouyre and I. Galand, Corrosion 42 1986, 54.
17. *Oriani, R. A. Hirth, J. P. Smailowski, M.* Hydrogen Degradation of Ferrous Metals. Noyes Publications, New Jersey, 1985, 822-852.
18. *Bernstein, I. M. Thomas, A. W.* Hydrogen Effects in Metals. Publication of the Metallurgical Society of AIME, Warrendale, 1983, 527-666.
19. *Deljusa, I.* Repair welding technik “half bead technik”. Croatian Welding Journal Zavarivanje 33, 1, 1990, 17-21

Acknowledgement. This publication is based on work sponsored by Croatian-American Joint Fund in cooperation with the Ministry of Science and Technology of Croatia and the National Institute of Standards and Technology (NIST) in the U.S.A. under project JF 137.